[Frontiers in Bioscience 12, 4267-4279, May 1, 2007]

Multimodality imaging of vascular endothelial growth factor and vascular endothelial growth factor receptor expression

Weibo Cai[1], Xiaoyuan Chen[1]

[1]The Molecular Imaging Program at Stanford (MIPS), Department of Radiology and Bio-X Program, Stanford University School of Medicine, Stanford, California

TABLE OF CONTENTS

1. ABSTRACT

Angiogenesis is a critical process in both physiological development and many pathological processes. Vascular endothelial growth factor (VEGF)/VEGF receptor (VEGFR) signaling pathway plays a pivotal role in regulating angiogenesis. Many therapeutic agents targeting VEGF and VEGFR are currently in preclinical and clinical development. The ability to quantitatively image VEGF/VEGFR expression in a non-invasive manner can aid in lesion detection, patient stratification, new drug development/validation, treatment monitoring, and dose optimization. It can also help in decide when or whether to start anti-angiogenic treatment targeting VEGF/VEGFR. This review summarizes the recent advances in multimodality imaging of VEGF/VEGFR expression using ultrasound, optical fluorescence, optical bioluminescence, SPECT, and PET in many diseases such as cancer, myocardial infarction, and ischemia. Much research effort will be needed in the future to improve the *in vivo* stability, tumor targeting efficacy, and pharmacokinetics of the imaging probes. With the development of new tracers with better targeting efficacy and desirable pharmacokinetics, clinical translation will be critical for the maximum benefit of VEGF/VEGFR targeted imaging agents.

2. VASCULAR ENDOTHELIAL GROWTH FACTOR (VEGF) AND VASCULAR ENDOTHELIAL GROWTH FACTOR RECEPTORS (VEGFRs)

Angiogenesis, the formation of new blood vessels, is a critical process in both physiological development and pathological processes such as tumor progression, wound healing, cardiovascular, inflammatory, ischemic, and infectious diseases (1-3). During adulthood, most blood vessels remain quiescent and angiogenesis occurs only in the cycling ovary and in the placenta during pregnancy. However, endothelial cells can restart to divide rapidly under physiological stimulus during malignant, inflammatory, and many other disorders. One of the most extensively studied angiogenesis-related signaling pathways is the VEGF/VEGFR interactions (4, 5). VEGF, a potent mitogen in embryonic and somatic angiogenesis, plays a pivotal role in both normal vascular tissue development and many disease processes (4, 6). The VEGF family is composed of seven members with a common VEGF homology domain: VEGF-A, VEGF-B, VEGF-C, VEGF-D, VEGF-E, VEGF-F, and placenta growth factor (5). VEGF-A is a dimeric, disulfide-bound glycoprotein existing in at least seven homodimeric isoforms, consisting of 121, 145, 148, 165, 183, 189, or 206 amino acids. Besides the difference in molecular weight, these isoforms

Table 1. Some therapeutic agents targeting VEGF or VEGFR currently in clinical development

Agent	Target	Company
Bevacizumab (Avastin)	VEGF	Genentech
VEGF-Trap	VEGF	Regeneron
SU5416	VEGFR	Sugen/Pharmacia
SU6668	VEGFR	Sugen/Pharmacia
SU11248	VEGFR	Sugen/Pharmacia
CP-547,632	VEGFR	Pfizer
PTK787	VEGFR	Novartis
ZD6474	VEGFR	Astra Zeneca
IMC-1C11	VEGFR	ImClone

also differ in their biological properties such as the ability to bind to cell surface heparin sulfate proteoglycans (5).

The angiogenic actions of VEGF are mainly mediated via two endothelium-specific receptor tyrosine kinases, Flt-1 (VEGFR-1) and Flk-1/KDR (VEGFR-2) (7). Both VEGFRs are largely restricted to vascular endothelial cells and all VEGF-A isoforms bind to both VEGFR-1 and VEGFR-2. It is now generally accepted that VEGFR-1 is critical for physiologic and developmental angiogenesis and its function varies with the stages of development, the states of physiologic and pathologic conditions, and the cell types in which it is expressed (5, 6). VEGFR-2 is the major mediator of the mitogenic, angiogenic, and permeability-enhancing effects of VEGF. Over-expression of VEGF and/or VEGFRs has been implicated as poor prognostic markers in various clinical studies (5). Agents that prevent VEGF-A binding to its receptors (8), antibodies that directly block VEGFR-2 (9, 10), and small molecules that inhibit the kinase activity of VEGFR-2 thereby block growth factor signaling (11-13), are all currently under active development. A selected list of therapeutic agents targeting VEGF or VEGFR in clinical trials are shown in Table 1 (14, 15). The critical role of VEGF-A in cancer progression has been highlighted by the approval of the humanized anti-VEGF monoclonal antibody bevacizumab (Avastin®; Genentech) for first line treatment (16). Development of VEGF- and VEGFR-targeted molecular imaging probes could serve as a new paradigm for the assessment of anti-angiogenic therapeutics and for better understanding the role and expression profile of VEGF/VEGFR in many angiogenesis-related diseases.

3. MOLECULAR IMAGING

Many imaging techniques have been routinely used to monitor the drug in blood, normal and tumor tissues and to evaluate the therapeutic effects (17, 18). Anatomical/functional imaging modalities such as computed tomography (CT), magnetic resonance imaging (MRI), and ultrasound have been used to assess the tumor size, tumor perfusion, integrity of the blood–brain barrier, vessel density, vessel permeability, blood oxygenation, blood volume, blood flow, blood velocity, and flow resistance (19-22). Recently, there has been a shift from conventional cytotoxic drugs to novel agents against specific molecular targets (e.g. VEGF/VEGFR) (23, 24). Such cytostatic therapies are much less toxic and disease stabilization may not lead to shrinkage of tumors in a short period of time. Thus, conventional imaging modalities are usually no longer adequate in evaluating the therapeutic efficacy as the data obtained are mostly anatomical and functional yet they do not convey enough information about the biological changes upon therapy at the molecular level. Molecular imaging, a recently emerged field, can play an important role in anti-angiogenic drug development and treatment monitoring processes.

Molecular imaging refers to the characterization and measurement of biological processes at the molecular level (25, 26). It takes advantage of the traditional diagnostic imaging techniques and introduces molecular probes to determine the expression of indicative molecular markers at different stages of diseases. Detection of these molecular markers can allow for much earlier diagnosis, earlier treatment, and better prognosis. Subsequent profiling to identify suitable treatment targets could lead to individualized therapy and treatment monitoring. Molecular imaging modalities includes molecular MRI, magnetic resonance spectroscopy (MRS), optical bioluminescence, optical fluorescence, targeted ultrasound, single photon emission computed tomography (SPECT), and positron emission tomography (PET; Figure 1) (26). Many hybrid systems that combine two or more of these modalities are already commercially available and certain others are under active development (27-29).

Since tumors are usually heterogeneous, tissue sampling does not always represent the biochemical or pathological processes of the disease. Temporal studies usually need large numbers of animals to be sacrificed at various time points to obtain statistically significant results. Molecular imaging can give whole body readout in an intact system; dramatically decrease the workload and reduce the cost during the drug development process; provide more statistically relevant results since longitudinal studies can be performed in the same animals; aid in early lesion detection in patients and patient stratification; and help in individualized treatment monitoring and dose optimization (30). To image and quantify biological processes *in vivo*, two requirements are needed: first, a molecular imaging probe composed of a label that can be detected with high sensitivity and a ligand that binds specifically and with high affinity to the target; and second, a sensitive, high-resolution imaging instrument to detect the signal non-invasively. In this review, we will summarize the progress to date on imaging VEGF/VEGFR expression. Besides cancer, other angiogenesis related diseases will also be briefly discussed (e.g. wound healing, myocardial infarction, ischemia, etc.).

4. *IN VIVO* IMAGING OF VEGF/VEGFR EXPRESSION

4.1. Magnetic resonance imaging

VEGF is the principal mediator of vascular permeability, which can be indirectly measured by dynamic contrast-enhanced MRI (DCE-MRI) and used as a pharmacodynamic end point for the development of new anti-angiogenic drugs. DCE-MRI is a non-invasive technique that can give parameters related to tissue perfusion and permeability (31). After the paramagnetic contrast agent (e.g. Gd-DTPA) is intravenously injected, it

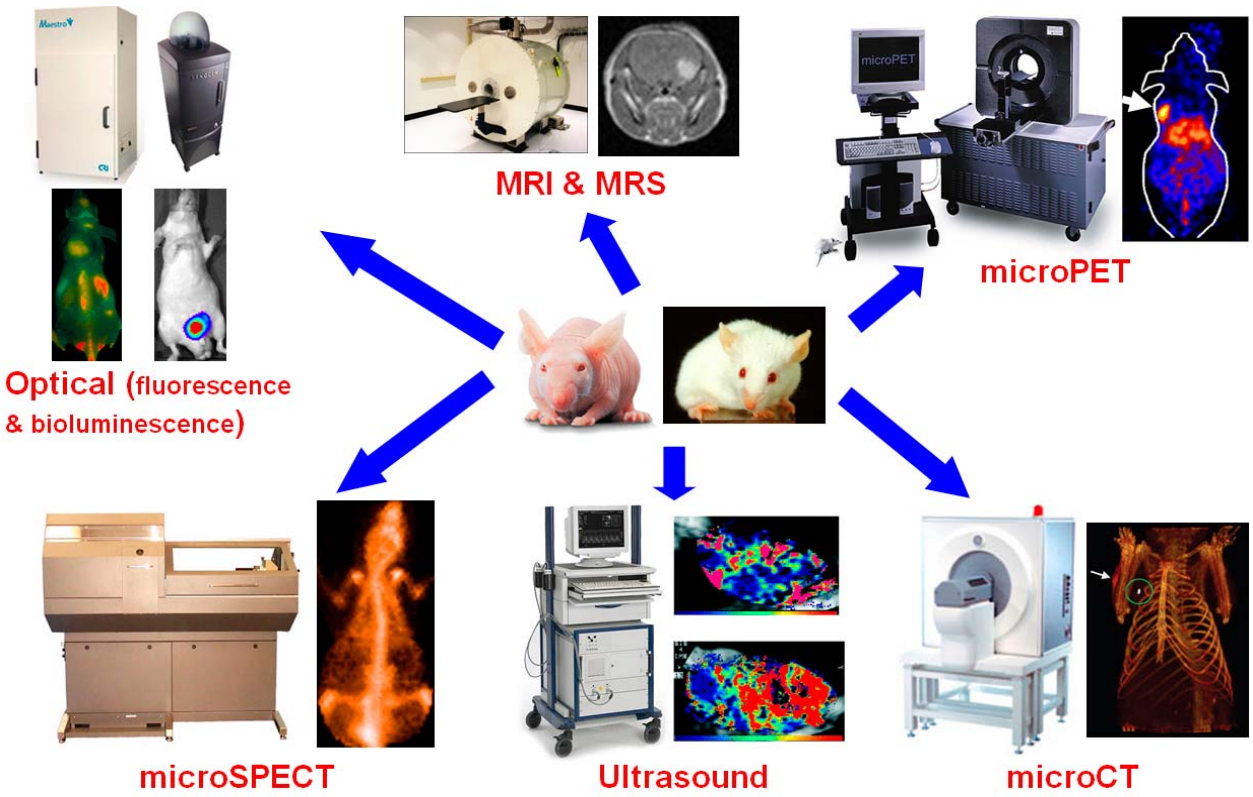

Figure 1. The multiple modalities for non-invasive small animal molecular imaging. Representative images of the instruments and resulting images are shown.

passes through tissues and diffuses out of the blood vessels. The signal intensity on T1-weighted images increases as the concentration of the contrast agent increases. Changes in signal intensity are recorded by serial images acquired before, during, and after the injection. Relative changes in semi-quantitative parameters, such as the maximum gradient of the signal increase and the maximum contrast enhancement, can be examined to reflect the physiologic end points of interest: tissue perfusion, vascular permeability, and vessel surface area (32-35). As a powerful tool for the rapid evaluation of acute pharmacodynamic effect of new anti-angiogenic drugs in clinical trials, DCE-MRI has often been used to examine the tumor vasculature.

Many reports have investigated the correlation of DCE-MRI measurements with immunohistological surrogates of tumor angiogenesis, such as microvessel density (MVD) based on CD31 staining and immunohistological staining of VEGF or other growth factors. In some cases the MRI parameters correlate with VEGF expression based on immunohistological staining (36-38), while in many other reports they do not (39-41). Taken together, analysis of DCE-MRI can reveal the *in vivo* VEGF expression level to a certain extent yet it may not be able to quantitatively measure VEGF/VEGFR expression non-invasively.

Molecular MRI (mMRI), in which contrast agent-mediated alteration of tissue relaxation times can allow for the detection and localization of molecular disease markers, recently emerged (42). MMRI can provide information at the molecular or cellular level, thus extending MRI further beyond the anatomical and physiological level. It is expected that in medical diagnostics, mMRI will pave the way toward a significant improvement in early detection of disease, therapy planning/monitoring and will therefore bring significant changes in patient management. MMRI has already been increasingly used in preclinical models to study tumor vasculature related targets such as integrin alpha(v)beta(3) (43-46). In these studies, the paramagnetic nanoparticles are coated with either antibodies or small peptidic/peptidomimetic integrin alpha(v)beta(3) antagonists. Such approach can also be employed for VEGFR imaging. The inherent low sensitivity of MRI can be improved by various contrast agents (47, 48). T1 agents (e.g. Gd^{3+}, Mn^{2+}) cause positive contrast enhancement (49, 50) while T2 agents (e.g. iron oxide) typically cause negative contrast enhancement (51). Thus, endogenous contrast can be used to obtain an image of an entire organism, and contrast agents can be labeled with specific targeting molecules so that they can reveal the expression status of the molecular target *in vivo*. Since mMRI itself is still in its infancy, no mMRI of VEGF or VEGFR expression has been reported to date although it is certainly feasible and deserves extensive investigation.

4.2. Ultrasound imaging

Because of its safety, low cost, ease of use, and wide availability, ultrasonography is the most commonly used clinical imaging modality (52). High-frequency sound waves are emitted from a transducer placed against the skin

and ultrasound images are obtained based on the sound wave reflected back from the internal organs. The contrast of ultrasound is dependent on the sound speed, sound attenuation, backscatter, and the imaging algorithm (53). Ultrasound can be used to image the microcirculation using both Doppler and microbubble methods (54). Power Doppler can be quantified to give an estimate of relative fractional vascular volume while microbubbles can show blood flow down to the microcirculation level by raising the signal from smaller vessels.

Using color Doppler imaging ultrasound, significant changes in blood flow in the murine renal cell carcinoma tumor feeding renal artery were observed under treatment with PTK787/ZK 222584, a VEGFR inhibitor (55). It was also demonstrated that blood flow measured by color Doppler imaging ultrasound correlates with the vessel density. In a human melanoma xenograft model, contrast-enhanced ultrasound measures of tumor neovascularity was compared with the expression of molecular markers of angiogenesis (56). After power Doppler and intermittent pulse-inversion harmonic imaging (PI-HI), the tumor tissues were surgically removed and sectioned in the same planes as the ultrasound images and immunohistochemical staining for VEGF were carried out. Although there is a trend of correlation between percent area stained with VEGF and intermittent PI-HI results, no statistical significance was achieved. In a follow-up study using similar approach in two melanoma models, linear regression analysis indicated statistically significant correlations between percent area stained with VEGF and power Doppler and intermittent PI-HI measures of tumor neovascularity (57). In rheumatoid arthritis, serum levels of VEGF at first presentation can predict the radiographic progression of disease over the subsequent year (58). Power Doppler ultrasonography has been used to demonstrate the presence of blood flow in small vessels and it was also found that the vascular signal correlates with histopathological quantification of the vascular density of synovial tissue (59). In all these studies, non-invasive ultrasound imaging results were compared with *ex vivo* VEGF staining results. Although good correlation was observed in many cases, these are not non-invasive imaging of VEGF expression. It is not until very recently that *in vivo* ultrasound imaging of VEGF/VEGFR expression was reported (60).

Since most contrast-enhanced ultrasound imaging uses microbubbles which are at least several micrometers in diameter, only the tumor endothelium can be targeted as these microbubbles are too large to extravasate (61). Thus, VEGFR is an excellent candidate for targeted untrasound imaging since it is almost exclusively expressed on activated endothelial cells (62). In a mouse model of pancreatic adenocarcinoma, targeted microbubbles were used to image and quantify vascular effects of two different anti-tumor therapies in both subcutaneous and orthotopic pancreatic tumors (60). Tumor-bearing mice were treated with anti-VEGF monoclonal antibodies and/or gemcitabine (a chemotherapy drug), and the localization of antibody-conjugated microbubbles to VEGFR-2 or VEGF-activated blood vessels (the VEGF-VEGFR complex) was monitored by contrast ultrasound (Figure 2). Significant signal enhancement of tumor vasculature was observed when compared with untargeted or control IgG-targeted microbubbles. Video intensity from targeted microbubbles also correlated with the expression level of the target (VEGFR-2 or the VEGF-VEGFR complex) and with MVD in tumors under therapy. This study demonstrated that targeted microbubbles can be a novel and attractive tool for non-invasive molecular imaging of tumor angiogenesis and for *in vivo* monitoring of vascular effects after therapy. In another report, we have imaged VEGFR-2 expression in two murine tumor models using anti-VEGFR2 monoclonal antibody conjugated microbubbles (63). Contrast-enhanced ultrasound imaging using targeted microbubbles showed significantly higher average video intensity compared with control microbubbles in both tumor models and video intensity was significantly lower when blocked by anti-VEGFR2 antibodies.

Ultrasound has relatively high spatial resolution (50-500 μm) yet it also has some disadvantages such as the relatively poor depth penetration (usually a few centimeters depending on the frequency used) and limited sensitivity (26). Further development of molecular imaging with ultrasound will likely involve the expansion of targeted diseases states, improvements in technology for ligand attachment to microbubbles, characterization of the acoustic behavior of targeted contrast agents, and development of better methods for imaging targeted ultrasound agents. Since acoustic destruction of "payload-bearing" microbubbles can be used to deliver drugs or to augment gene transfection (64), angiogenesis-targeted microbubbles may also have applications in site-specific therapy for ischemic tissues or tumors.

4.3. Optical (fluorescence and bioluminescence) imaging

Optical imaging is a relatively low-cost method suitable primarily for small animal study. In fluorescence imaging, excitation light illuminates the subject, and a charge-coupled device (CCD) camera collects the emission light at a shifted wavelength (26). The fluorescent probe can be either injected or genetically engineered and no substrate is required for its visualization. The drawback is that these systems are typically not quantitative, and the image information is surface-weighted due to tissue absorption (25). In most cases significant background signal is also observed because of tissue autofluorescence.

In a transgenic mouse model where a VEGF promoter was chosen to drive a GFP reporter gene, VEGF expression during wound healing and possible impairment of wound healing due to collateral tissue damage was imaged *in vivo* (65). Mice received two full thickness incisions in the dorsal skin: one with the free electron laser (FEL) and one with a scalpel. Afterwards, mice were imaged for GFP expression at multiple time points. It was found that GFP expression peaked at 2-3 weeks after surgery and FEL lesions exhibited more total GFP expression than scalpel lesions. This pioneering study demonstrated the feasibility of using transgenic mice carrying photoactive reporter genes for studying cellular process in a non-invasive manner.

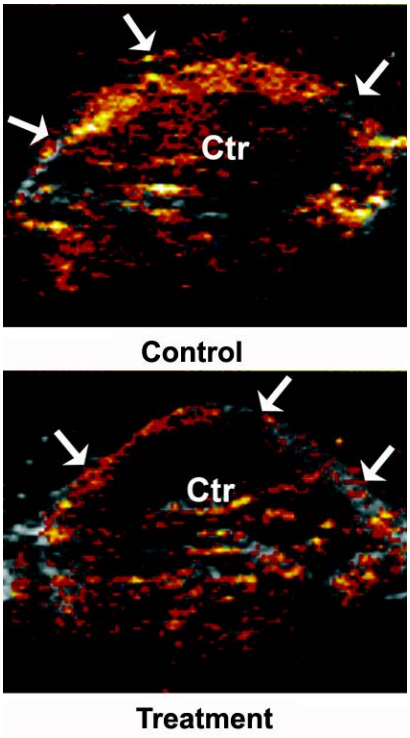

Figure 2. Contrast ultrasound images obtained using microbubbles targeted to VEGFR-2 in control and treated animals. Video intensity is significantly lower in mice under anti-VEGF treatment. Arrows indicate the periphery of the tumor and "Ctr" denotes the center of the tumor. Reproduced with permission from ref. 60.

Another component of optical imaging is bioluminescence imaging (BLI), which can be used to detect very low levels of signal because the emitted light is virtually background free (66). BLI does not require an external light source. Instead, it detects light that is emitted from within the experimental animals through the action of an enzyme (usually luciferase) on its substrate (e.g. D-luciferin). Non-invasive indirect imaging of VEGF expression with BLI in living transgenic mice has also been reported, where a two-step transcriptional amplification approach was used to augment the transcriptional activity of the relatively weak VEGF promoter (67). VEGF gene expression was imaged in both a wound-healing model and a subcutaneous mammary tumor model (Figure 3). The BLI signal had good correlation with the endogenous VEGF protein levels in the wound tissue. This method provided another means for longitudinal monitoring of VEGF induction during wound healing and tumor progression. The transgenic mouse model developed in this study may also be useful in various other applications where non-invasive monitoring of VEGF gene expression is needed.

The major disadvantage of optical imaging in living subjects is the poor tissue penetration of light. Due to the limited penetration and intense scattering of light, optical imaging will only be possible in humans in limited sites such as the tissues and lesions close to the skin surface, tissues accessible by endoscopy, and intraoperative visualization (68). Near-infrared (NIR, 700 – 900 nm) approaches can provide better opportunities for preclinical evaluation in small animal models since the absorbance spectra for all biomolecules reach minima in the NIR region which provides a clear window for *in vivo* optical imaging (69).

Human VEGF was conjugated to a self-assembled "dock and lock" system and retained its functional activities (70). After incorporating an additional cysteine residue for site-specific modification, a NIR fluorescent dye Cy5.5 (maximum emission 696 nm) was conjugated and the resulting Cy5.5-VEGF was used for *in vivo* imaging. Although tumor contrast was observed after administration of the probe, no information was reported about the whole body distribution of Cy5.5-VEGF (70, 71). This self-assembled "dock and lock" system may provide new opportunities of generating labeled functionally active proteins for other biomedical purposes (72).

Another approach to fluorescence imaging of deeper structures uses fluorescence-mediated tomography (FMT) (73). The subject is exposed to continuous wave or pulsed light from different sources, and multiple detectors arranged in a spatially defined order in an imaging chamber are used to capture the emitted light. Mathematical processing of the collected data gives the reconstructed tomographic image. In mouse tumor models, FMT has been used to prospectively determine the feasibility of imaging vascular volume fraction (VVF) and its therapeutic inhibition after intravenous administration of long-circulating NIR fluorescent blood pool agents (74). VVFs of the tumors could be depicted with *in vivo* imaging in three dimensions within less than 5 minutes of data acquisition time and less than 3 minutes of analysis. Such approach has the potential to facilitate future small animal VEGF/VEGFR imaging in deeper tissues.

4.4. Single-photon emission computed tomography imaging

As its name suggests (single photon emission), the source of SPECT images are gamma ray emissions (75). Internal radiation is administered through a low mass amount of pharmaceutical labeled with a radioactive isotope. When the radioactive isotope decays, it emits gamma rays which can be detected by a gamma camera. The gamma camera can be used in planar imaging to obtain 2-D images, or in SPECT imaging to obtain 3-D images. A collimator is used to only allow the emitted gamma photon to travel along certain directions to reach the detector, which ensures that the position on the detector accurately represents the source of the gamma ray. SPECT imaging has a very low detection efficiency ($<10^{-4}$ times the emitted number of gamma rays) because of the use of lead collimators to define the angle of incidence (76). The major advantage of SPECT imaging is that it can be used for simultaneous imaging of multiple radionuclides since the gamma ray emitted from different radioisotopes can be differentiated based on the energy (77).

Recombinant human $VEGF_{121}$ was labeled with ^{111}In for identification of ischemic tissue in a rabbit model, where unilateral hind-limb ischemia was created by

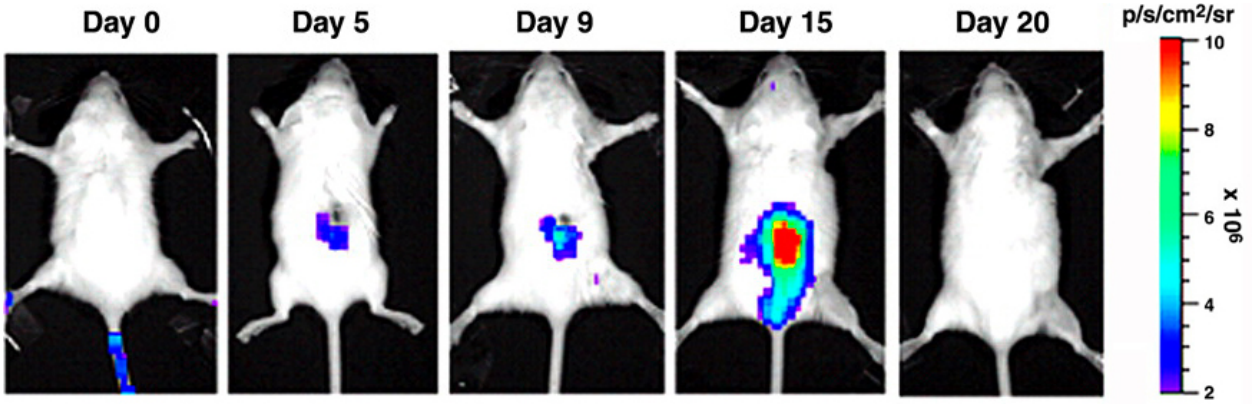

Figure 3. Induction of luciferase expression (driven by a VEGF promotor) in a transgenic mouse during wound healing. Mouse was imaged before and after wound creation using D-luciferin as the substrate. Reproduced with permission from ref. 67.

femoral artery excision (78). Some contrast was observed between the ischemic and the contralateral hindlimbs. Since previous studies in many endothelial cell lines have demonstrated high number of VEGFRs per hypoxic cell (79) and *in vitro* studies also revealed substantial VEGFR-specific binding of the ^{111}In-labeled $VEGF_{121}$, the authors attributed the subtle difference in ischemic muscle versus normal muscle uptake to technical factors and low sensitivity of the pinhole collimator. $VEGF_{121}$ has also been labeled with ^{99m}Tc through an "adapter/docking" strategy and the tracer was tested in a 4T1 murine mammary carcinoma with tumor uptake of about 3 %ID/g (72, 80). It was concluded that this ^{99m}Tc-labeled $VEGF_{121}$ is stable for about 1 h *in vivo* and can be used to image mouse tumor neovasculature in lesions as small as several millimeters in soft tissue (Figure 4A). Recently, it was also used to image tumor vasculature before and after different types of chemotherapy (81).

^{123}I-$VEGF_{165}$ has also been reported as a potential tumor marker (82). Despite the high receptor affinity of this tracer, biodistribution in A2508 melanoma tumor-bearing mice indicated low tumor-to-background ratio, likely due to the low metabolic stability of the compound. Nonetheless, biodistribution, safety, and absorbed dose of ^{123}I-$VEGF_{165}$ was studied in nine patients with pancreatic carcinoma (83). Following intravenous administration, sequential images were recorded during the initial 30 min post-injection (p.i.). Although the majority of primary pancreatic tumors and their metastases were visualized by ^{123}I-$VEGF_{165}$ scans, the organ with the highest absorbed dose was the thyroid due to severe deiodination. Another report evaluated the usefulness of ^{123}I-$VEGF_{165}$ for tumor localization in gastrointestinal cancer patients (84). Dynamic acquisition was initiated immediately after injection and carried out until 30 min p.i. All patients then underwent SPECT imaging at 1.5 h p.i. By comparing the SPECT results with CT and MRI, the primary and metastatic lesions were identified in some patients by ^{123}I-$VEGF_{165}$ SPECT. Recently, ^{125}I-labeled $VEGF_{121}$ and $VEGF_{165}$ have also been used for biodistribution and autoradiography studies (85). As with most other radioiodinated tracers, prominent activity accumulation in the stomach was observed due to deiodination. Interestingly, ^{125}I-$VEGF_{121}$ accumulation in tumors decreased with increasing tumor volume suggesting that small tumors have high VEGFR expression than large tumors. It was also found that ^{125}I-$VEGF_{165}$ uptake was greater than that of ^{125}I-$VEGF_{121}$ in some organs (e.g. kidney, heart, and lung) but lower in the other organs. The reasons for different accumulation in these organs remain unclear although it was hypothesized to be related to the different expression level of VEGFR-1 and VEGFR-2 in these organs, since $VEGF_{165}$ binds to VEGFR-1 with higher affinity than VEGFR-2 (86, 87).

A recombinant protein composed of $VEGF_{165}$ fused through a flexible polypeptide G_4S linker to the n-lobe of human transferrin (hnTf-VEGF) was reported for imaging angiogenesis (88). The molecular weight of hnTf-VEGF is 65 kDa and 130 kDa for the monomer and dimer, respectively. ^{111}In-hnTf-VEGF accumulated in U87MG human glioblastoma tumors (6.7 %ID/g at 72 h p.i.) and the tumor uptake decreased when co-injected with 100-fold excess of VEGF but not with apotransferrin (Figure 4B). HnTf-VEGF represents a prototypic protein harboring the metal-binding site of transferrin for labeling with ^{111}In without the need to introduce metal chelators.

Due to the soluble and more dynamic nature of VEGF, imaging VEGF expression is very difficult. Thus all the abovementioned reports used radiolabeled VEGF isoforms for SPECT imaging of VEGFR expression. Although the VEGF isoforms used in these studies all exist in nature and should have very strong binding affinity and specificity to VEGFRs, much research is needed in the future to improve the *in vivo* stability, target affinity/specificity, and pharmacokinetics of these radiopharmaceuticals. Another imaging modality, PET, may offer many advantages over SPECT and the increasing popularity of the clinical PET and PET/CT scanners can significantly facilitate clinical translation of promising new tracers (27, 89).

4.5. Positron emission tomography imaging

PET uses positron-labeled molecules in very low mass amounts to image and measure the function of biological processes with minimal disturbance (90, 91).

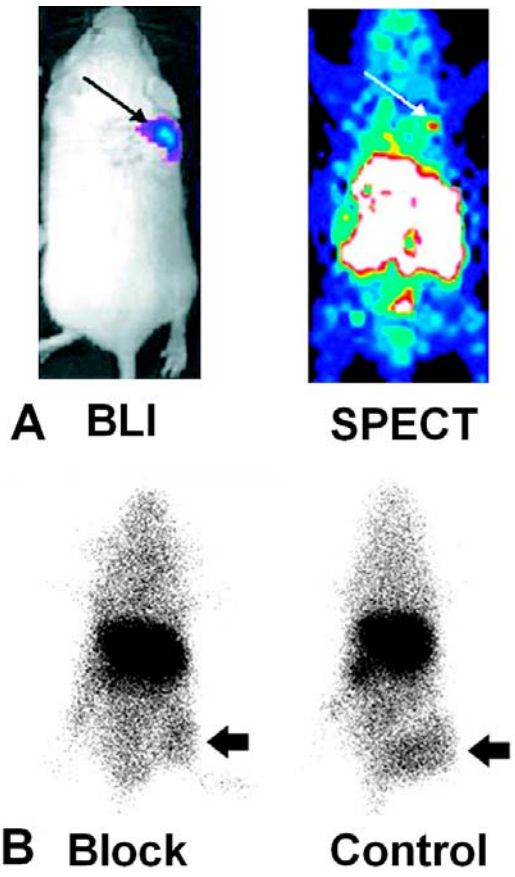

Figure 4. SPECT imaging of VEGFR expression. (A) BLI (after injection of D-luciferin) and SPECT imaging (after injection of ^{99m}Tc-labeled VEGF$_{121}$) of a mouse with right shoulder tumor. The tumor cells were transfected with firefly luciferase. (B) Posterior whole-body images of an athymic tumor-bearing mouse at 48 h after injection of ^{111}In-labeled hnTf-VEGF. "Block" denotes co-administration of 100-fold excess of unlabeled apotransferrin. Arrows indicate tumors in all cases. Reproduced with permission from refs. 80, 88.

With the development of microPET scanners dedicated to small animal imaging studies, it can provide a similar *in vivo* imaging capability in mice, rats, monkeys, and humans so one can readily transfer knowledge and molecular measurements between species (92, 93). A few radiolabeled anti-VEGF antibodies have been reported. VG76e, an IgG1 monoclonal antibody that binds to human VEGF, was labeled with ^{124}I for PET imaging of solid tumor xenografts in immune-deficient mice (94). Whole-animal PET imaging studies revealed a high tumor-to-background contrast (Figure 5A). Although VEGF specificity *in vivo* was demonstrated in this report, the poor immunoreactivity (< 35%) of the radiolabeled antibody limits the potential use of this tracer. HuMV833, the humanized version of a mouse monoclonal anti-VEGF antibody MV833, was also labeled with ^{124}I and the distribution and biological effects of HuMV833 in patients in a phase I clinical trial were investigated (95). Patients with progressive solid tumors were treated with various doses of HuMV833 and PET imaging using ^{124}I-HuMV833 was carried out to measure the antibody distribution in and clearance from tissues. It was found that antibody distribution and clearance were quite heterogeneous not only between and within patients but also between and within individual tumors, suggesting that intra-patient dose escalation approaches or more precisely defined patient cohorts would be preferred in the design of phase I studies with anti-angiogenic antibodies like HuMV833.

We have labeled VEGF$_{121}$ with ^{64}Cu ($t_{1/2}$ = 12.7 h) for PET imaging of tumor angiogenesis and VEGFR expression (96). DOTA-VEGF$_{121}$ (where DOTA denotes 1,4,7,10-tetraazacyclododecane-1,4,7,10-tetraacetic acid) exhibited nano-molar receptor binding affinity (comparable to VEGF$_{121}$) *in vitro*. MicroPET imaging revealed rapid, specific, and prominent uptake of ^{64}Cu-DOTA-VEGF$_{121}$ (~ 15%ID/g) in highly vascularized small U87MG tumor with high VEGFR-2 expression but significantly lower and sporadic uptake (~ 3%ID/g) in large U87MG tumor with low VEGFR-2 expression (Figure 5B). Western blotting of tumor tissue lysate, immunofluorescence staining, and blocking studies with unlabeled VEGF$_{121}$ confirmed that the tumor uptake is VEGFR specific. This is the first report on PET imaging of VEGFR expression. This study also demonstrated the dynamic nature of VEGFR expression during tumor progression in that even for the same tumor model, VEGFR expression level can be dramatically different at different stages. Successful demonstration of the ability of ^{64}Cu-DOTA-VEGF$_{121}$ to visualize VEGFR expression *in vivo* should allow for clinical translation of this tracer to image tumor angiogenesis and to guide VEGFR-targeted cancer therapy.

In a follow-up study, a VEGFR-2 specific fusion toxin VEGF$_{121}$/rGel (composed of VEGF$_{121}$ linked with a G_4S tether to recombinant plant toxin gelonin) was used to treat orthotopic glioblastoma in a mouse model (97). Before initiation of treatment, microPET imaging with ^{64}Cu-labeled VEGF$_{121}$/rGel was performed to evaluate the tumor targeting efficacy and the pharmacokinetics. It was found that ^{64}Cu-DOTA-VEGF$_{121}$/rGel exhibited high tumor accumulation/retention and high tumor-to-background contrast up to 48 h after injection in glioblastoma xenografts (Figure 5C). Based on the *in vivo* pharmacokinetics of ^{64}Cu-DOTA-VEGF$_{121}$/rGel, VEGF$_{121}$/rGel was administered every other day for the treatment of orthotopic U87MG glioblastomas. Such study of tumor targeting efficacy and pharmacokinetics using radiolabeled drugs demonstrated the power of molecular imaging, where cancer patients can also be selected for specific molecular cancer therapy based on pre-treatment screening using a radiolabeled drug or drug analog. After initiation of treatment, the therapeutic efficacy of VEGF$_{121}$/rGel was monitored by non-invasive BLI, MRI, and PET imaging. PET with ^{18}F-FLT (measures tumor proliferation) revealed significant decrease in tumor proliferation in VEGF$_{121}$/rGel-treated mice compared with the control mice. Histologic analysis revealed specific tumor neovasculature damage after treatment with 4 doses

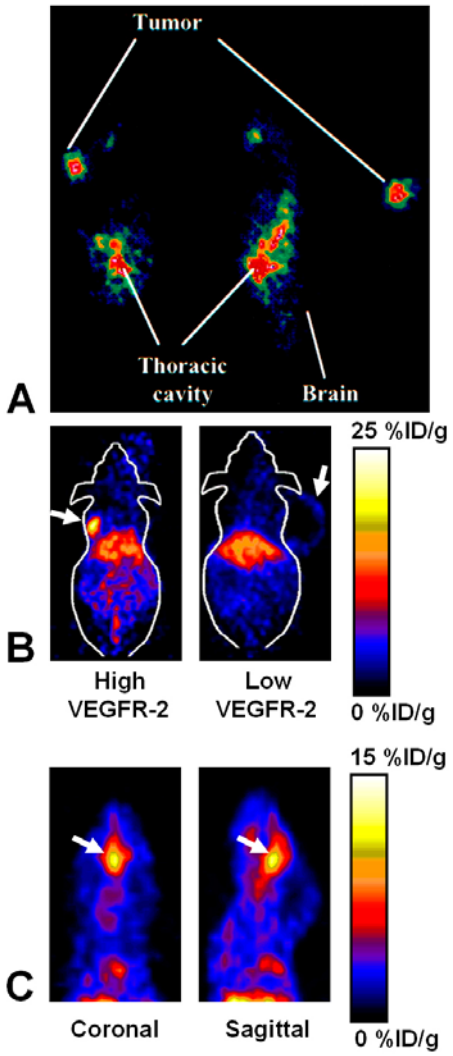

Figure 5. PET imaging of VEGF/VEGFR expression. (A) PET images of a tumor-bearing mouse at 24 h after injection of ^{124}I-labeled VG76e. Left to right, coronal, sagittal, and transverse views. (B) MicroPET images of U87MG tumor-bearing mice at 16 h after injection of ^{64}Cu-DOTA-VEGF$_{121}$. (C) MicroPET images of orthotopic U87MG tumor-bearing mice at 18 h after injection of ^{64}Cu-DOTA-VEGF$_{121}$/rGel. %ID/g: percent injected dose per gram of tissue. Arrows indicate tumors. Reproduced with permission from refs. 94, 96-97.

of VEGF$_{121}$/rGel, which was also non-invasively revealed by a significant decrease in peak BLI tumor signal intensity. Successful non-invasive monitoring of treatment efficacy by multimodality imaging suggested that future clinical multimodality imaging and therapy with VEGF$_{121}$/rGel may provide an effective means to prospectively identify patients who will benefit from VEGF$_{121}$/rGel therapy and then stratify, personalize, and monitor treatment to obtain optimal survival outcomes.

^{64}Cu was also used to site-specifically label VEGF$_{121}$ and it was found that PEGylation showed considerably prolonged blood clearance (72). Compared with ^{99m}Tc-labeled analog where the tumor uptake (~ 2 %ID/g) was lower than most of the normal organs and the kidney uptake was about 120 %ID/g, the PEGylated version gave higher tumor uptake (~ 2.5 %ID/g) and lower kidney uptake at about 65 %ID/g (72).

PET imaging using radiolabeled VEGF can also play a role in other angiogenesis-related diseases besides cancer. Myocardial infarction (MI) can lead to the activation of many biological pathways including VEGF/VEGFR signaling (98, 99). Using the previously validated PET tracer ^{64}Cu-DOTA-VEGF$_{121}$, for the first time we imaged the kinetics of VEGFR expression in living subjects with MI in a rat model (100). MI was induced by ligation of the left anterior descending coronary artery in Sprague-Dawley rats and confirmed by ultrasound. ^{64}Cu-DOTA-VEGF$_{121}$ PET scans were performed prior to MI induction, and at days 3, 10, 17, and 24 after MI induction. Baseline myocardial uptake of ^{64}Cu-DOTA-VEGF$_{121}$ was minimal (0.3 ± 0.1 %ID/g). After MI, ^{64}Cu-DOTA-VEGF$_{121}$ myocardial uptake significantly increased (up to 1.0 ± 0.1 %ID/g) and was elevated for 2 weeks, after which it returned to baseline levels.

MicroPET imaging has also been used to monitor the transgene expression, function, and effects in the rat MI model (101). Adenovirus with cytomegalovirus promoter driving a VEGF gene linked to a PET reporter gene herpes simplex virus type 1 mutant thymidine kinase (Ad-CMV-VEGF$_{121}$-CMV-HSV1-sr39tk) was constructed. After MI induction, Ad-CMV-VEGF$_{121}$-CMV-HSV1-sr39tk was injected at the peri-infarct region. Non-invasive microPET imaging was used to assess the uptake of 9-(4-[^{18}F]-fluorohydroxymethylbutyl) guanine ([^{18}F]-FHBG, a substrate of HSV1-sr39tk) PET reporter probe by cells expressing the HSV1-sr39tk PET reporter gene (102, 103). It was found that *in vivo* reporter gene expression measured by microPET correlated well with myocardial tissue HSV1-sr39tk enzyme activity and myocardial tissue VEGF level. Although no significant improvements in functional parameters such as myocardial contractility, perfusion, and metabolism was achieved, this report established the feasibility of molecular imaging for monitoring angiogenic gene expression with a PET reporter gene and probe non-invasively, quantitatively, and repetitively.

PET imaging of other angiogenesis related disease models (e.g. ischemia) is also currently ongoing in our laboratory. In a hindlimb ischemia model, PET imaging showed significantly higher ^{64}Cu-DOTA-VEGF$_{121}$ uptake in ischemic hindlimbs than in non-ischemic hindlimbs (104). To test the specificity of the radiotracer, sham-operated hindlimbs were also scanned and the radiotracer uptake was not significantly different from non-ischemic hindlimbs. Treadmill exercise training was also found to increase ^{64}Cu-DOTA-VEGF$_{121}$ uptake in ischemic hindlimbs compared with non-exercised hindlimbs.

All VEGF-A isoforms bind to both VEGFR-1 and VEGFR-2 (5). In the imaging studies reported to date, specificity to either VEGFR-1 or VEGFR-2 has rarely been

achieved as most of the tracers are based on VEGF isoforms. Kidney has high VEGFR-1 expression which can take up VEGF-A based tracer thus usually makes it the dose limiting organ (96, 105). Alanine-scanning mutagenesis has been used to identify a positively charged surface in $VEGF_{165}$ that mediates the binding to VEGFR-2 (106). Arg^{82}, Lys^{84}, and His^{86}, located in a hairpin loop, were found to be critical for binding VEGFR-2, while negatively charged residues, Asp^{63}, Glu^{64}, and Glu^{67}, were associated with VEGFR-1 binding. Mutations in the 63-67 region of VEGF exhibited only modest effects on VEGFR-2 binding but significant reduction in affinity with VEGFR-1. As $VEGF_{121}$ is a soluble, non-heparin-binding variant that exists in solution as a disulfide-linked homodimer containing the full biological and receptor-binding activity of the larger variants (5), we are in the process of developing VEGFR-1 and VEGFR-2 specific VEGF mutants based on $VEGF_{121}$.

Comparing all the modalities used for VEGF/VEGFR imaging, PET is the most-widely studied. With the development of new tracers with better targeting efficacy and desirable pharmacokinetics, clinical translation will be critical for the maximum benefit of VEGF-based imaging agents. Peptidic VEGFR antagonists can be labeled with ^{11}C or ^{18}F and they may allow for higher throughput than antibody- or protein-based radiotracers, as one hour post-injection is usually sufficient for a peptide-based tracer to clear from the non-targeted organs and give high contrast PET images (107). It can take several hours and even days before high contrast PET images can be obtained for antibody-based tracers (108, 109).

5. SUMMARY AND PERSPECTIVE

Multimodality imaging of VEGF/VEGFR expression has been reported using a variety of strategies (e.g. protein, antibody, reporter gene-based) for many diseases (e.g. cancer, MI, and ischemia). Non-invasive imaging has been used not only for lesion detection, but also for monitoring the therapeutic efficacy, both being the major goals of molecular imaging. In some cases, angiogenesis is inhibited and in other cases angiogenesis is promoted to improve the physiological outcome. Despite the critical role of VEGF and VEGFR in angiogenesis, *in vivo* imaging of VEGF/VEGFR expression has been surprisingly understudied. In the clinical setting, the right timing can be critical for VEGFR-targeted cancer therapy and non-invasive imaging of VEGF/VEGFR can help in determining whether to start and when to start VEGFR-targeted treatment.

Almost exclusively, the strategy used for VEGF imaging uses either anti-VEGF antibodies or reporter gene approaches. Due to the soluble and dynamic nature of VEGF proteins, imaging VEGF expression was not as extensively studied as imaging VEGFR expression. Most reports on imaging VEGFR expression used the naturally occurring VEGF isoforms. Further improvement of VEGF-based imaging probes can be achieved in many ways. First, site-specific labeling may be advantageous than labeling on Lysine residues in terms of retaining the binding affinity and functional activity. Second, VEGFR-2 specific tracers can be developed. VEGFR-2 is the target of many anti-angiogenic therapies and it is generally accepted to be more functionally important than VEGFR-1 in many diseases including cancer (5, 62, 110). The ability to image VEGFR-2 *in vivo* by PET using mutant VEGF-based tracers could be a valuable tool for evaluation of patients with a variety of malignancies, particularly for monitoring those undergoing anti-angiogenic therapies targeting VEGFR-2. Third, peptide or small molecule-based tracers may be developed. High affinity peptide binders to VEGFR-2 have been reported using phage display and certainly deserve further investigation (111).

Molecular imaging has enormous potential in clinical applications since the imaging and therapeutic targets are usually the same. The molecular imaging field grows extremely fast over the last decade and it is getting more widely accepted by pharmaceutical companies. It is expected that in the foreseeable future molecular imaging will be routinely applied in many steps of the anti-angiogenic drug development process. The combination of molecular and anatomical/functional imaging techniques in assessing tumor angiogenesis and in response to anti-angiogenic therapy will be a powerful tool. The new generation clinical PET/CT and microPET/microCT, as well as PET/MRI currently in active development (29, 89, 112), will likely play a major role in molecular imaging of angiogenesis for the years to come.

6. ACKNOWLEDGMENT

This work was partially supported by National Institute of Biomedical Imaging and Bioengineering (NIBIB) (R21 EB001785), National Cancer Institute (NCI) (R21 CA102123, P50 CA114747, and R24 CA93862), Department of Defense (DOD) (W81XWH-04-1-0697, W81XWH-06-1-0665, W81XWH-06-1-0042, and DAMD17-03-1-0143), and a Benedict Cassen Postdoctoral Fellowship from the Education and Research Foundation of the Society of Nuclear Medicine (W.Cai).

7. REFERENCES

1. J. Folkman: Angiogenesis in cancer, vascular, rheumatoid and other disease. *Nat Med* 1, 27-31 (1995)
2. G. Bergers, L.E. Benjamin: Tumorigenesis and the angiogenic switch. *Nat Rev Cancer* 3, 401-10 (2003)
3. P. Carmeliet: Angiogenesis in life, disease and medicine. *Nature* 438, 932-6 (2005)
4. N. Ferrara: VEGF and the quest for tumour angiogenesis factors. *Nat Rev Cancer* 2, 795-803 (2002)
5. N. Ferrara: Vascular endothelial growth factor: basic science and clinical progress. *Endocr Rev* 25, 581-611 (2004)
6. N. Ferrara: The role of VEGF in the regulation of physiological and pathological angiogenesis. *EXS*, 209-31 (2005)
7. D.J. Hicklin, L.M. Ellis: Role of the vascular endothelial growth factor pathway in tumor growth and angiogenesis. *J Clin Oncol* 23, 1011-27 (2005)
8. J. Sun, D.A. Wang, R.K. Jain, A. Carie, S. Paquette, E. Ennis, M.A. Blaskovich, L. Baldini, D. Coppola, A.D.

Hamilton, S.M. Sebti: Inhibiting angiogenesis and tumorigenesis by a synthetic molecule that blocks binding of both VEGF and PDGF to their receptors. *Oncogene* 24, 4701-9 (2005)
9. H. Watanabe, A.J. Mamelak, B. Wang, B.G. Howell, I. Freed, C. Esche, M. Nakayama, G. Nagasaki, D.J. Hicklin, R.S. Kerbel, D.N. Sauder: Anti-vascular endothelial growth factor receptor-2 (Flk-1/KDR) antibody suppresses contact hypersensitivity. *Exp Dermatol* 13, 671-81 (2004)
10. M. Prewett, J. Huber, Y. Li, A. Santiago, W. O'Connor, K. King, J. Overholser, A. Hooper, B. Pytowski, L. Witte, P. Bohlen, D.J. Hicklin: Antivascular endothelial growth factor receptor (fetal liver kinase 1) monoclonal antibody inhibits tumor angiogenesis and growth of several mouse and human tumors. *Cancer Res* 59, 5209-18 (1999)
11. F. Ciardiello, R. Caputo, V. Damiano, T. Troiani, D. Vitagliano, F. Carlomagno, B.M. Veneziani, G. Fontanini, A.R. Bianco, G. Tortora: Antitumor effects of ZD6474, a small molecule vascular endothelial growth factor receptor tyrosine kinase inhibitor, with additional activity against epidermal growth factor receptor tyrosine kinase. *Clin Cancer Res* 9, 1546-56 (2003)
12. S.R. Wedge, D.J. Ogilvie, M. Dukes, J. Kendrew, J.O. Curwen, L.F. Hennequin, A.P. Thomas, E.S. Stokes, B. Curry, G.H. Richmond, P.F. Wadsworth: ZD4190: an orally active inhibitor of vascular endothelial growth factor signaling with broad-spectrum antitumor efficacy. *Cancer Res* 60, 970-5 (2000)
13. J.M. Wood, G. Bold, E. Buchdunger, R. Cozens, S. Ferrari, J. Frei, F. Hofmann, J. Mestan, H. Mett, T. O'Reilly, E. Persohn, J. Rosel, C. Schnell, D. Stover, A. Theuer, H. Towbin, F. Wenger, K. Woods-Cook, A. Menrad, G. Siemeister, M. Schirner, K.H. Thierauch, M.R. Schneider, J. Drevs, G. Martiny-Baron, F. Totzke: PTK787/ZK 222584, a novel and potent inhibitor of vascular endothelial growth factor receptor tyrosine kinases, impairs vascular endothelial growth factor-induced responses and tumor growth after oral administration. *Cancer Res* 60, 2178-89 (2000)
14. F.A. Eskens: Angiogenesis inhibitors in clinical development; where are we now and where are we going? *Br J Cancer* 90, 1-7 (2004)
15. N. Ferrara, K.J. Hillan, H.P. Gerber, W. Novotny: Discovery and development of bevacizumab, an anti-VEGF antibody for treating cancer. *Nat Rev Drug Discov* 3, 391-400 (2004)
16. G. Middleton, D.V. Lapka: Bevacizumab (Avastin). *Clin J Oncol Nurs* 8, 666-9 (2004)
17. S.J. Gwyther: New imaging techniques in cancer management. *Ann Oncol* 16 Suppl 2, ii63-70 (2005)
18. M. Rudin, R. Weissleder: Molecular imaging in drug discovery and development. *Nat Rev Drug Discov* 2, 123-31 (2003)
19. E. Bagarinao, T. Nakai, Y. Tanaka: Real-time functional MRI: development and emerging applications. *Magn Reson Med Sci* 5, 157-65 (2006)
20. J.W. Prichard, L.M. Brass: New anatomical and functional imaging methods. *Ann Neurol* 32, 395-400 (1992)
21. P. Dawson: Functional imaging in CT. *Eur J Radiol* 60, 331-40 (2006)
22. J.A. Detre: Clinical applicability of functional MRI. *J Magn Reson Imaging* 23, 808-15 (2006)
23. R. Kerbel, J. Folkman: Clinical translation of angiogenesis inhibitors. *Nat Rev Cancer* 2, 727-39 (2002)
24. M. Cristofanilli, C. Charnsangavej, G.N. Hortobagyi: Angiogenesis modulation in cancer research: novel clinical approaches. *Nat Rev Drug Discov* 1, 415-26 (2002)
25. R. Weissleder, U. Mahmood: Molecular imaging. *Radiology* 219, 316-33 (2001)
26. T.F. Massoud, S.S. Gambhir: Molecular imaging in living subjects: seeing fundamental biological processes in a new light. *Genes Dev* 17, 545-80 (2003)
27. T. Beyer, D.W. Townsend, T. Brun, P.E. Kinahan, M. Charron, R. Roddy, J. Jerin, J. Young, L. Byars, R. Nutt: A combined PET/CT scanner for clinical oncology. *J Nucl Med* 41, 1369-79 (2000)
28. E. Even-Sapir, H. Lerman, G. Lievshitz, A. Khafif, D.M. Fliss, A. Schwartz, E. Gur, Y. Skornick, S. Schneebaum: Lymphoscintigraphy for sentinel node mapping using a hybrid SPECT/CT system. *J Nucl Med* 44, 1413-20 (2003)
29. C. Catana, Y. Wu, M.S. Judenhofer, J. Qi, B.J. Pichler, S.R. Cherry: Simultaneous acquisition of multislice PET and MR images: initial results with a MR-compatible PET scanner. *J Nucl Med* 47, 1968-76 (2006)
30. W. Cai, J. Rao, S.S. Gambhir, X. Chen: How molecular imaging is speeding up anti-angiogenic drug development. *Mol Cancer Ther* 5, 2624-33 (2006)
31. A.P. Pathak, B. Gimi, K. Glunde, E. Ackerstaff, D. Artemov, Z.M. Bhujwalla: Molecular and functional imaging of cancer: Advances in MRI and MRS. *Methods Enzymol* 386, 3-60 (2004)
32. P.L. Choyke, A.J. Dwyer, M.V. Knopp: Functional tumor imaging with dynamic contrast-enhanced magnetic resonance imaging. *J Magn Reson Imaging* 17, 509-20 (2003)
33. F. Kiessling, B. Morgenstern, C. Zhang: Contrast agents and applications to assess tumor angiogenesis *in vivo* by magnetic resonance imaging. *Curr Med Chem* 14, 77-91 (2007)
34. J.P. O'Connor, A. Jackson, G.J. Parker, G.C. Jayson: DCE-MRI biomarkers in the clinical evaluation of antiangiogenic and vascular disrupting agents. *Br J Cancer* 96, 189-95 (2007)
35. A.R. Padhani, J.E. Husband: Dynamic contrast-enhanced MRI studies in oncology with an emphasis on quantification, validation and human studies. *Clin Radiol* 56, 607-20 (2001)
36. R. Matsubayashi, Y. Matsuo, G. Edakuni, T. Satoh, O. Tokunaga, S. Kudo: Breast masses with peripheral rim enhancement on dynamic contrast-enhanced MR images: correlation of MR findings with histologic features and expression of growth factors. *Radiology* 217, 841-8 (2000)
37. B.H. Hoang, J.P. Dyke, J.A. Koutcher, A.G. Huvos, H. Mizobuchi, B.A. Mazza, R. Gorlick, J.H. Healey: VEGF expression in osteosarcoma correlates with vascular permeability by dynamic MRI. *Clin Orthop Relat Res*, 32-8 (2004)
38. M.V. Knopp, E. Weiss, H.P. Sinn, J. Mattern, H. Junkermann, J. Radeleff, A. Magener, G. Brix, S. Delorme, I. Zuna, G. van Kaick: Pathophysiologic basis of contrast

enhancement in breast tumors. *J Magn Reson Imaging* 10, 260-6 (1999)
39. M.Y. Su, Y.C. Cheung, J.P. Fruehauf, H. Yu, O. Nalcioglu, E. Mechetner, A. Kyshtoobayeva, S.C. Chen, S. Hsueh, C.E. McLaren, Y.L. Wan: Correlation of dynamic contrast enhancement MRI parameters with microvessel density and VEGF for assessment of angiogenesis in breast cancer. *J Magn Reson Imaging* 18, 467-77 (2003)
40. H. Hawighorst, P.G. Knapstein, M.V. Knopp, W. Weikel, G. Brix, I. Zuna, S.O. Schonberg, M. Essig, P. Vaupel, G. van Kaick: Uterine cervical carcinoma: comparison of standard and pharmacokinetic analysis of time-intensity curves for assessment of tumor angiogenesis and patient survival. *Cancer Res* 58, 3598-602 (1998)
41. B. Wang, Z.Q. Gao, X. Yan: Correlative study of angiogenesis and dynamic contrast-enhanced magnetic resonance imaging features of hepatocellular carcinoma. *Acta Radiol* 46, 353-8 (2005)
42. D.E. Sosnovik, R. Weissleder: Emerging concepts in molecular MRI. *Curr Opin Biotechnol* 18, 4-10 (2007)
43. D.A. Sipkins, D.A. Cheresh, M.R. Kazemi, L.M. Nevin, M.D. Bednarski, K.C. Li: Detection of tumor angiogenesis *in vivo* by alpha(v)beta(3)-targeted magnetic resonance imaging. *Nat Med* 4, 623-6 (1998)
44. P.M. Winter, A.M. Morawski, S.D. Caruthers, R.W. Fuhrhop, H. Zhang, T.A. Williams, J.S. Allen, E.K. Lacy, J.D. Robertson, G.M. Lanza, S.A. Wickline: Molecular imaging of angiogenesis in early-stage atherosclerosis with alpha(v)beta(3)-integrin-targeted nanoparticles. *Circulation* 108, 2270-4 (2003)
45. P.M. Winter, S.D. Caruthers, A. Kassner, T.D. Harris, L.K. Chinen, J.S. Allen, E.K. Lacy, H. Zhang, J.D. Robertson, S.A. Wickline, G.M. Lanza: Molecular imaging of angiogenesis in nascent Vx-2 rabbit tumors using a novel alpha(v)beta(3)-targeted nanoparticle and 1.5 tesla magnetic resonance imaging. *Cancer Res* 63, 5838-43 (2003)
46. A.H. Schmieder, P.M. Winter, S.D. Caruthers, T.D. Harris, T.A. Williams, J.S. Allen, E.K. Lacy, H. Zhang, M.J. Scott, G. Hu, J.D. Robertson, S.A. Wickline, G.M. Lanza: Molecular MR imaging of melanoma angiogenesis with alpha(v)beta(3)-targeted paramagnetic nanoparticles. *Magn Reson Med* 53, 621-7 (2005)
47. R.G. Pautler, S.E. Fraser: The year(s) of the contrast agent - micro-MRI in the new millennium. *Curr Opin Immunol* 15, 385-92 (2003)
48. Z. Zhang, S.A. Nair, T.J. McMurry: Gadolinium meets medicinal chemistry: MRI contrast agent development. *Curr Med Chem* 12, 751-78 (2005)
49. S. Aime, C. Cabella, S. Colombatto, S. Geninatti Crich, E. Gianolio, F. Maggioni: Insights into the use of paramagnetic Gd(III) complexes in MR-molecular imaging investigations. *J Magn Reson Imaging* 16, 394-406 (2002)
50. A.C. Silva, J.H. Lee, I. Aoki, A.P. Koretsky: Manganese-enhanced magnetic resonance imaging (MEMRI): methodological and practical considerations. *NMR Biomed* 17, 532-43 (2004)
51. D.L. Thorek, A.K. Chen, J. Czupryna, A. Tsourkas: Superparamagnetic iron oxide nanoparticle probes for molecular imaging. *Ann Biomed Eng* 34, 23-38 (2006)
52. S.H. Bloch, P.A. Dayton, K.W. Ferrara: Targeted imaging using ultrasound contrast agents. Progess and opportunities for clinical and research applications. *IEEE Eng Med Biol Mag* 23, 18-29 (2004)
53. M.H. Wink, H. Wijkstra, J.J. De La Rosette, C.A. Grimbergen: Ultrasound imaging and contrast agents: a safe alternative to MRI? *Minim Invasive Ther Allied Technol* 15, 93-100 (2006)
54. H.D. Liang, M.J. Blomley: The role of ultrasound in molecular imaging. *Br J Radiol* 76 Spec No 2, S140-50 (2003)
55. J. Drevs, I. Hofmann, H. Hugenschmidt, C. Wittig, H. Madjar, M. Muller, J. Wood, G. Martiny-Baron, C. Unger, D. Marme: Effects of PTK787/ZK 222584, a specific inhibitor of vascular endothelial growth factor receptor tyrosine kinases, on primary tumor, metastasis, vessel density, and blood flow in a murine renal cell carcinoma model. *Cancer Res* 60, 4819-24 (2000)
56. F. Forsberg, A.P. Dicker, M.L. Thakur, N.M. Rawool, J.B. Liu, W.T. Shi, L.N. Nazarian: Comparing contrast-enhanced ultrasound to immunohistochemical markers of angiogenesis in a human melanoma xenograft model: preliminary results. *Ultrasound Med Biol* 28, 445-51 (2002)
57. F. Forsberg, R.J. Ro, M. Potoczek, J.B. Liu, C.R. Merritt, K.M. James, A.P. Dicker, L.N. Nazarian: Assessment of angiogenesis: implications for ultrasound imaging. *Ultrasonics* 42, 325-30 (2004)
58. G. Salvador, R. Sanmarti, B. Gil-Torregrosa, A. Garcia-Peiro, J.R. Rodriguez-Cros, J.D. Canete: Synovial vascular patterns and angiogenic factors expression in synovial tissue and serum of patients with rheumatoid arthritis. *Rheumatology (Oxford)* 45, 966-71 (2006)
59. P.C. Taylor: Serum vascular markers and vascular imaging in assessment of rheumatoid arthritis disease activity and response to therapy. *Rheumatology (Oxford)* 44, 721-8 (2005)
60. G. Korpanty, J.G. Carbon, P.A. Grayburn, J.B. Fleming, R.A. Brekken: Monitoring response to anticancer therapy by targeting microbubbles to tumor vasculature. *Clin Cancer Res* 13, 323-30 (2007)
61. G. Korpanty, P.A. Grayburn, R.V. Shohet, R.A. Brekken: Targeting vascular endothelium with avidin microbubbles. *Ultrasound Med Biol* 31, 1279-83 (2005)
62. T.L. Underiner, B. Ruggeri, D.E. Gingrich: Development of vascular endothelial growth factor receptor (VEGFR) kinase inhibitors as anti-angiogenic agents in cancer therapy. *Curr Med Chem* 11, 731-45 (2004)
63. J.K. Willmann, R. Paulmurugan, K. Chen, O. Gheysens, M. Rodriguez-Porcel, A.M. Lutz, I.Y. Chen, X. Chen, S.S. Gambhir: Ultrasonic imaging of tumor angiogenesis with contrast microbubbles targeted to vascular endothelial growth factor type 2 receptor. *Radiology*, revision (2007)
64. R.V. Shohet, S. Chen, Y.T. Zhou, Z. Wang, R.S. Meidell, R.H. Unger, P.A. Grayburn: Echocardiographic destruction of albumin microbubbles directs gene delivery to the myocardium. *Circulation* 101, 2554-6 (2000)
65. A.D. Izzo, M.A. Mackanos, J.T. Beckham, E.D. Jansen: *In vivo* optical imaging of expression of vascular endothelial growth factor following laser incision in skin. *Lasers Surg Med* 29, 343-50 (2001)
66. R.S. Negrin, C.H. Contag: *In vivo* imaging using bioluminescence: a tool for probing graft-versus-host disease. *Nat Rev Immunol* 6, 484-90 (2006)

67. Y. Wang, M. Iyer, A. Annala, L. Wu, M. Carey, S.S. Gambhir: Noninvasive indirect imaging of vascular endothelial growth factor gene expression using bioluminescence imaging in living transgenic mice. *Physiol Genomics* 24, 173-80 (2006)
68. W. Cai, D.W. Shin, K. Chen, O. Gheysens, Q. Cao, S.X. Wang, S.S. Gambhir, X. Chen: Peptide-labeled near-infrared quantum dots for imaging tumor vasculature in living subjects. *Nano Lett* 6, 669-76 (2006)
69. J.V. Frangioni: *In vivo* near-infrared fluorescence imaging. *Curr Opin Chem Biol* 7, 626-34 (2003)
70. M.V. Backer, V. Patel, B.T. Jehning, J.M. Backer: Self-assembled "dock and lock" system for linking payloads to targeting proteins. *Bioconjug Chem* 17, 912-9 (2006)
71. M.V. Backer, T.I. Gaynutdinov, V. Patel, A.K. Bandyopadhyaya, B.T. Thirumamagal, W. Tjarks, R.F. Barth, K. Claffey, J.M. Backer: Vascular endothelial growth factor selectively targets boronated dendrimers to tumor vasculature. *Mol Cancer Ther* 4, 1423-9 (2005)
72. M.V. Backer, Z. Levashova, V. Patel, B.T. Jehning, K. Claffey, F.G. Blankenberg, J.M. Backer: Molecular imaging of VEGF receptors in angiogenic vasculature with single-chain VEGF-based probes. *Nat Med*, (2007)
73. X. Montet, V. Ntziachristos, J. Grimm, R. Weissleder: Tomographic fluorescence mapping of tumor targets. *Cancer Res* 65, 6330-6 (2005)
74. X. Montet, J.L. Figueiredo, H. Alencar, V. Ntziachristos, U. Mahmood, R. Weissleder: Tomographic fluorescence imaging of tumor vascular volume in mice. *Radiology* 242, 751-8 (2007)
75. K. Peremans, B. Cornelissen, B. Van Den Bossche, K. Audenaert, C. Van de Wiele: A review of small animal imaging planar and pinhole spect Gamma camera imaging. *Vet Radiol Ultrasound* 46, 162-70 (2005)
76. A.F. Chatziioannou: Instrumentation for molecular imaging in preclinical research: Micro-PET and Micro-SPECT. *Proc Am Thorac Soc* 2, 533-6, 10-11 (2005)
77. D.S. Berman, H. Kiat, K. Van Train, J.D. Friedman, F.P. Wang, G. Germano: Dual-isotope myocardial perfusion SPECT with rest thallium-201 and stress Tc-99m sestamibi. *Cardiol Clin* 12, 261-70 (1994)
78. E. Lu, W.R. Wagner, U. Schellenberger, J.A. Abraham, A.L. Klibanov, S.R. Woulfe, M.M. Csikari, D. Fischer, G.F. Schreiner, G.H. Brandenburger, F.S. Villanueva: Targeted *in vivo* labeling of receptors for vascular endothelial growth factor: approach to identification of ischemic tissue. *Circulation* 108, 97-103 (2003)
79. H. Thieme, L.P. Aiello, H. Takagi, N. Ferrara, G.L. King: Comparative analysis of vascular endothelial growth factor receptors on retinal and aortic vascular endothelial cells. *Diabetes* 44, 98-103 (1995)
80. F.G. Blankenberg, S. Mandl, Y.A. Cao, C. O'Connell-Rodwell, C. Contag, C. Mari, T.I. Gaynutdinov, J.L. Vanderheyden, M.V. Backer, J.M. Backer: Tumor imaging using a standardized radiolabeled adapter protein docked to vascular endothelial growth factor. *J Nucl Med* 45, 1373-80 (2004)
81. F.G. Blankenberg, M.V. Backer, Z. Levashova, V. Patel, J.M. Backer: *In vivo* tumor angiogenesis imaging with site-specific labeled 99mTc-HYNIC-VEGF. *Eur J Nucl Med Mol Imaging* 33, 841-8 (2006)
82. B. Cornelissen, R. Oltenfreiter, V. Kersemans, L. Staelens, F. Frankenne, J.M. Foidart, G. Slegers: *In vitro* and *in vivo* evaluation of [^{123}I]-VEGF$_{165}$ as a potential tumor marker. *Nucl Med Biol* 32, 431-6 (2005)
83. S. Li, M. Peck-Radosavljevic, O. Kienast, J. Preitfellner, E. Havlik, W. Schima, T. Traub-Weidinger, S. Graf, M. Beheshti, M. Schmid, P. Angelberger, R. Dudczak: Iodine-123-vascular endothelial growth factor-165 (^{123}I-VEGF$_{165}$). Biodistribution, safety and radiation dosimetry in patients with pancreatic carcinoma. *Q J Nucl Med Mol Imaging* 48, 198-206 (2004)
84. S. Li, M. Peck-Radosavljevic, O. Kienast, J. Preitfellner, G. Hamilton, A. Kurtaran, C. Pirich, P. Angelberger, R. Dudczak: Imaging gastrointestinal tumours using vascular endothelial growth factor-165 (VEGF$_{165}$) receptor scintigraphy. *Ann Oncol* 14, 1274-7 (2003)
85. M. Yoshimoto, S. Kinuya, A. Kawashima, R. Nishii, K. Yokoyama, K. Kawai: Radioiodinated VEGF to image tumor angiogenesis in a LS180 tumor xenograft model. *Nucl Med Biol* 33, 963-9 (2006)
86. T.P. Quinn, K.G. Peters, C. De Vries, N. Ferrara, L.T. Williams: Fetal liver kinase 1 is a receptor for vascular endothelial growth factor and is selectively expressed in vascular endothelium. *Proc Natl Acad Sci USA* 90, 7533-7 (1993)
87. Y. Yamazaki, T. Morita: Molecular and functional diversity of vascular endothelial growth factors. *Mol Divers* 10, 515-27 (2006)
88. C. Chan, J. Sandhu, A. Guha, D.A. Scollard, J. Wang, P. Chen, K. Bai, L. Lee, R.M. Reilly: A human transferrin-vascular endothelial growth factor (hnTf-VEGF) fusion protein containing an integrated binding site for ^{111}In for imaging tumor angiogenesis. *J Nucl Med* 46, 1745-52 (2005)
89. D.W. Townsend, T. Beyer: A combined PET/CT scanner: the path to true image fusion. *Br J Radiol* 75 Spec No, S24-30 (2002)
90. M.E. Phelps, E.J. Hoffman, N.A. Mullani, M.M. Ter-Pogossian: Application of annihilation coincidence detection to transaxial reconstruction tomography. *J Nucl Med* 16, 210-24 (1975)
91. M.E. Phelps: PET: the merging of biology and imaging into molecular imaging. *J Nucl Med* 41, 661-81 (2000)
92. S.R. Cherry, Y. Shao, R.W. Silverman, K. Meadors, S. Siegel, A. Chatziioannou, J.W. Young, W.F. Jones, J.C. Moyers, D. Newport, A. Boutefnouchet, T.H. Farquhar, M. Andreaco, M.J. Paulus, D.M. Binkley, R. Nutt, M.E. Phelps: MicroPET: a high resolution PET scanner for imaging small animals. *IEEE Trans Nucl Sci* 44, 1161-6 (1997)
93. A.F. Chatziioannou, S.R. Cherry, Y. Shao, R.W. Silverman, K. Meadors, T.H. Farquhar, M. Pedarsani, M.E. Phelps: Performance evaluation of microPET: a high-resolution lutetium oxyorthosilicate PET scanner for animal imaging. *J Nucl Med* 40, 1164-75 (1999)
94. D.R. Collingridge, V.A. Carroll, M. Glaser, E.O. Aboagye, S. Osman, O.C. Hutchinson, H. Barthel, S.K. Luthra, F. Brady, R. Bicknell, P. Price, A.L. Harris: The development of [^{124}I]iodinated-VG76e: a novel tracer for imaging vascular endothelial growth factor *in vivo* using positron emission tomography. *Cancer Res* 62, 5912-9 (2002)
95. G.C. Jayson, J. Zweit, A. Jackson, C. Mulatero, P. Julyan, M. Ranson, L. Broughton, J. Wagstaff, L.

Hakannson, G. Groenewegen, J. Bailey, N. Smith, D. Hastings, J. Lawrance, H. Haroon, T. Ward, A.T. McGown, M. Tang, D. Levitt, S. Marreaud, F.F. Lehmann, M. Herold, H. Zwierzina: Molecular imaging and biological evaluation of HuMV833 anti-VEGF antibody: implications for trial design of antiangiogenic antibodies. *J Natl Cancer Inst* 94, 1484-93 (2002)
96. W. Cai, K. Chen, K.A. Mohamedali, Q. Cao, S.S. Gambhir, M.G. Rosenblum, X. Chen: PET of vascular endothelial growth factor receptor expression. *J Nucl Med* 47, 2048-56 (2006)
97. A.R. Hsu, W. Cai, A. Veeravagu, K.A. Mohamedali, K. Chen, S. Kim, H. Vogel, L.C. Hou, V. Tse, M.G. Rosenblum, X. Chen: Multimodality molecular imaging of glioblastoma growth inhibition with vasculature-targeting fusion toxin $VEGF_{121}$/rGel. *J Nucl Med* 48, 445-54 (2007)
98. J. Li, L.F. Brown, M.G. Hibberd, J.D. Grossman, J.P. Morgan, M. Simons: VEGF, flk-1, and flt-1 expression in a rat myocardial infarction model of angiogenesis. *Am J Physiol* 270, H1803-11 (1996)
99. T. Soeki, Y. Tamura, H. Shinohara, H. Tanaka, K. Bando, N. Fukuda: Serial changes in serum VEGF and HGF in patients with acute myocardial infarction. *Cardiology* 93, 168-74 (2000)
100. M. Rodriguez-Porcel, W. Cai, O. Gheysens, I.Y. Chen, K. Chen, L. He, J.K. Willman, J.C. Wu, Z.B. Li, K.A. Mohamedali, M.G. Rosenblum, X. Chen, S.S. Gambhir: Imaging of VEGF receptor in a rat myocardial infarction model using positron emission tomography. *J Nucl Med*, submitted (2007)
101. J.C. Wu, I.Y. Chen, Y. Wang, J.R. Tseng, A. Chhabra, M. Salek, J.J. Min, M.C. Fishbein, R. Crystal, S.S. Gambhir: Molecular imaging of the kinetics of vascular endothelial growth factor gene expression in ischemic myocardium. *Circulation* 110, 685-91 (2004)
102. M.M. Alauddin, P.S. Conti: Synthesis and preliminary evaluation of 9-(4-[^{18}F]-fluoro-3-hydroxymethylbutyl)guanine ([^{18}F]FHBG): a new potential imaging agent for viral infection and gene therapy using PET. *Nucl Med Biol* 25, 175-80 (1998)
103. S. Yaghoubi, J.R. Barrio, M. Dahlbom, M. Iyer, M. Namavari, N. Satyamurthy, R. Goldman, H.R. Herschman, M.E. Phelps, S.S. Gambhir: Human pharmacokinetic and dosimetry studies of [^{18}F]FHBG: a reporter probe for imaging herpes simplex virus type-1 thymidine kinase reporter gene expression. *J Nucl Med* 42, 1225-34 (2001)
104. J.K. Willmann, W. Cai, R. Paulmurugan, K. Chen, O. Gheysens, M. Rodriguez-Porcel, A.M. Lutz, I.Y. Chen, X. Chen, S.S. Gambhir: Molecular imaging of therapeutic angiogenesis in murine hindlimb ischemia using PET and ^{64}Cu-labeled vascular endothelial growth factor121. submitted (2007)
105. M. Simon, W. Rockl, C. Hornig, E.F. Grone, H. Theis, H.A. Weich, E. Fuchs, A. Yayon, H.J. Grone: Receptors of vascular endothelial growth factor/vascular permeability factor (VEGF/VPF) in fetal and adult human kidney: localization and [^{125}I]VEGF binding sites. *J Am Soc Nephrol* 9, 1032-44 (1998)
106. B.A. Keyt, H.V. Nguyen, L.T. Berleau, C.M. Duarte, J. Park, H. Chen, N. Ferrara: Identification of vascular endothelial growth factor determinants for binding KDR and FLT-1 receptors. Generation of receptor-selective VEGF variants by site-directed mutagenesis. *J Biol Chem* 271, 5638-46 (1996)
107. W. Cai, X. Zhang, Y. Wu, X. Chen: A thiol-reactive ^{18}F-labeling agent, *N*-[2-(4-^{18}F-fluorobenzamido)ethyl]maleimide (^{18}F-FBEM), and the synthesis of RGD peptide-based tracer for PET imaging of alpha(v)beta(3) integrin expression. *J Nucl Med* 47, 1172-80 (2006)
108. W. Cai, Y. Wu, K. Chen, Q. Cao, D.A. Tice, X. Chen: *In vitro* and *in vivo* characterization of ^{64}Cu-labeled Abegrin^{TM}, a humanized monoclonal antibody against integrin alpha(v)beta(3). *Cancer Res* 66, 9673-81 (2006)
109. W. Cai, K. Chen, L. He, Q. Cao, A. Koong, X. Chen: Quantitative PET of EGFR expression in xenograft-bearing mice using ^{64}Cu-labeled cetuximab, a chimeric anti-EGFR monoclonal antibody. *Eur J Nucl Med Mol Imaging*, (2007)
110. C. Gridelli, A. Rossi, P. Maione: New antiangiogenetic agents and non-small cell lung cancer. *Crit Rev Oncol Hematol* 60, 76-86 (2006)
111. A. Shrivastava, M.A. von Wronski, A.K. Sato, D.T. Dransfield, D. Sexton, N. Bogdan, R. Pillai, P. Nanjappan, B. Song, E. Marinelli, D. DeOliveira, C. Luneau, M. Devlin, A. Muruganandam, A. Abujoub, G. Connelly, Q.L. Wu, G. Conley, Q. Chang, M.F. Tweedle, R.C. Ladner, R.E. Swenson, A.D. Nunn: A distinct strategy to generate high-affinity peptide binders to receptor tyrosine kinases. *Protein Eng Des Sel* 18, 417-24 (2005)
112. Y. Shao, S.R. Cherry, K. Farahani, K. Meadors, S. Siegel, R.W. Silverman, P.K. Marsden: Simultaneous PET and MR imaging. *Phys Med Biol* 42, 1965-70 (1997)

Abbreviations: VEGF: vascular endothelial growth factor; VEGFR: vascular endothelial growth factor receptor; CT: computed tomography; MRI: magnetic resonance imaging; MRS: magnetic resonance spectroscopy; BLI: bioluminescence imaging; SPECT: single photon emission computed tomography; PET: positron emission tomography; DCE-MRI: dynamic contrast-enhanced MRI; MVD: microvessel density; mMRI: molecular MRI; PI-HI: pulse-inversion harmonic imaging; CCD: charge-coupled device; FEL: free electron laser; GFP: green fluorenscence protein; NIR: near-infrared; FMT: fluorescence-mediated tomography; VVF: vascular volume fraction; DOTA: 1,4,7,10-tetraazacyclododecane-1,4,7,10-tetraacetic acid; rGel: gelonin; %ID/g: percentage injected dose per gram of tissue; MI: myocardial infarction; [^{18}F]-FHBG: 9-(4-[^{18}F]-fluorohydroxymethylbutyl) guanine

Key Words: Molecular imaging, VEGF, VEGFR, Angiogenesis, Positron emission tomography, Review

Send correspondence to: Xiaoyuan Chen, PhD, the Molecular Imaging Program at Stanford (MIPS), Department of Radiology and Bio-X Program, Stanford University School of Medicine, 1201 Welch Rd, P095, Stanford, CA 94305, Tel: 650-725-0950, Fax: 650-736-7925, E-mail: shawchen@stanford.edu

http://www.bioscience.org/current/vol12.htm